An Analytical Theory of Harmonic Distortion in RC Networks with Voltage-Dependent Capacitance

A Charge-Conserving Small-Nonlinearity Analysis Through the Fifth Harmonic

Boris F. Kuznetsov, Professor, Doctor of Technical Sciences

Central Asian Institute of Engineering, Dentistry and Medicine (CAEDMI)

Bishkek, Kyrgyzstan

Abstract

Class II ceramic capacitors, including X7R and X5R MLCCs, are widely used in compact analog and mixed-signal hardware. Their main advantage is high volumetric capacitance, but that advantage comes from nonlinear dielectric materials. As a result, the effective capacitance depends on the applied voltage. In decoupling and bulk filtering applications, this effect is often treated mainly as a loss of capacitance under DC bias [4], [5], [6]. In signal-path circuits, however, voltage-dependent capacitance has a deeper consequence: the capacitor becomes a nonlinear charge-storage element and can generate harmonic distortion [1], [2], [3].

This paper studies the simplest circuit in which the mechanism appears clearly: a first-order RC low-pass network with a voltage-dependent shunt capacitor. Despite its simplicity, this network is a useful model for many practical nodes, including anti-alias filters, ADC input networks, AC-coupling stages, and local analog filters. The central question is practical: why does the distortion peak near the transition region of the filter rather than at the highest signal frequency?

The analysis is based on a charge-conserving capacitor model. The nonlinear capacitor is described by its charge-voltage relation $Q(V)$, not by an instantaneous capacitance value inserted into an otherwise linear current law. The differential capacitance is $C_d(V) = dQ/dV$, and the capacitor current is $i = dQ(V)/dt$. This distinction matters because the common shortcut $Q = C(V)V$ can describe a different physical component when $C(V)$ is actually a differential capacitance [7], [8], [9].

The resulting small-nonlinearity RC equation contains nonlinear terms of the form $v\dot{v}$, $v^2\dot{v}$, $v^3\dot{v}$, and $v^4\dot{v}$. This structure explains the frequency dependence of the distortion. At low frequencies, the voltage across the capacitor is large, but its time derivative is small. At high frequencies, the derivative can be large, but the capacitor voltage and the generated harmonics are attenuated by the RC network. The distortion therefore peaks between these two limits.

For the second harmonic, a compact closed-form expression is obtained, with a maximum at $\Omega = 1/\sqrt{2}$, or approximately $0.707 f_c$. For the direct third-harmonic mechanism, the maximum occurs near $0.458 f_c$. For the fourth and fifth harmonics, a recursive analytical formulation is given in terms of complex Fourier coefficients and harmonic balance. The theory provides a foundation for analyzing Class II ceramic capacitors in precision analog signal paths, SAR ADC front ends, and other systems where passive-component nonlinearity can limit dynamic range [11], [12], [14].

Keywords: voltage-dependent capacitance, Class II ceramic capacitor, MLCC, X7R, X5R, RC filter, harmonic distortion, THD, charge-conserving model, differential capacitance, harmonic balance.

1. Introduction

In everyday circuit design, a capacitor is often treated as a simple passive element. If a schematic shows a 10 nF capacitor, the first-order assumption is that the capacitance is constant. For many jobs this is good enough. It gives quick estimates of time constants, cutoff frequencies, ripple, and filtering margin.

That assumption becomes risky when the capacitor is placed in a precision analog signal path and sees a significant AC voltage swing. This is especially true for Class II multilayer ceramic capacitors. X7R, X5R, and related dielectrics provide high dielectric constant and small package size, but their capacitance can vary substantially with applied voltage [4], [5], [6]. Such a capacitor is not a linear charge-storage element.

This behavior is usually discussed as the DC bias effect. Designers learn that the effective capacitance at the operating voltage can be much smaller than the nominal value. That is already important for filters and power supplies. In signal-path applications there is a second issue. If the voltage across the capacitor changes with time, the differential capacitance changes with it. The capacitor current is then no longer a linear function of dv/dt. This produces harmonic distortion [1], [2], [3].

The simplest example is a first-order RC low-pass filter. In the linear case, this network does not generate harmonics. A sinusoidal input produces a sinusoidal output with a different amplitude and phase. If the shunt capacitor has voltage-dependent capacitance, the situation changes. During each cycle, the capacitor moves through different parts of its charge-voltage curve. The charge and discharge rates depend on the instantaneous voltage, and the output waveform is no longer a pure sine wave.

It is tempting to assume that this distortion should simply increase with frequency. After all, capacitor current is related to the voltage derivative, and the derivative of a sine wave is proportional to frequency. That argument captures only half of the problem. In an RC low-pass filter, the voltage across the capacitor decreases at high frequency. The second, third, and higher harmonics also appear at 2ω, 3ω, and above, where the same filter attenuates them even more. The frequency-dependent current generation competes with the falling capacitor voltage and with the filtering of the generated harmonics.

This leads to the key physical result: the largest harmonic distortion is not expected at arbitrarily high frequency. It occurs in a finite transition region of the network, near the cutoff frequency, where both the capacitor voltage and the capacitor current are appreciable.

The goal of this paper is to obtain that result analytically. The analysis is not based on numerical simulation or an empirical rule. Instead, it develops a small-nonlinearity theory for an RC network with a voltage-dependent capacitor. The resulting expressions show where the second, third, fourth, and fifth harmonics come from, which coefficients of the capacitance-voltage curve control them, and why the frequency maximum appears near the transition band of the filter.

2. Background and Related Work

Voltage-dependent capacitance in Class II ceramic capacitors is well known. Manufacturers commonly publish capacitance versus DC bias data. X7R and X5R parts can show a strong dependence, while C0G/NP0 parts are usually far more stable [4], [5], [6]. This is the basis for the common design rule: use C0G/NP0, film, or another low-distortion dielectric in critical analog signal paths [3].

Knowing that the DC bias effect exists is not enough for distortion analysis. Loss of nominal capacitance shifts the filter time constant. Nonlinearity of the charge-voltage relation changes the waveform. These effects are related, but they are not the same. Harmonic analysis depends on the shape of $Q(V)$, or equiv-

alently the shape of the differential capacitance $C_d(V)$, over the signal swing, not just on the capacitance at one bias point [7], [8].

Engineering articles have already shown that high-k ceramic capacitors can produce measurable distortion in audio circuits, anti-alias filters, amplifier feedback networks, and ADC input paths [1], [2], [3]. Measurements show that replacing X7R or X5R capacitors with C0G/NP0 parts can substantially reduce THD [1], [3]. This confirms that the effect is not merely academic.

Many practical discussions stop at component selection. They answer which capacitor to use, but they do not always explain analytically where in frequency the distortion should be worst. They also often mix two separate issues: physically correct modeling of a nonlinear capacitor and calculation of the harmonics generated in the circuit.

For correct modeling, the charge-based formulation is essential. If the differential capacitance is known, the charge is obtained by integration [7], [8]:

$$Q(V) = Q(V_0) + \int_{V_0}^{V} C_d(u)\, du.$$

The current is then

$$i(t) = \frac{dQ(V)}{dt}.$$

If instead one writes $Q(V) = C(V)V$ while $C(V)$ is intended to be a differential capacitance, the model changes. Its derivative is

$$\frac{dQ}{dV} = C(V) + V\frac{dC}{dV},$$

which is not equal to the specified $C(V)$ in general. That mistake can change the predicted harmonics [7], [8].

This paper therefore starts from a specific modeling choice: first write the physically consistent charge equation for the RC network, and only then perform the small-nonlinearity analysis. This makes the result suitable for later validation in SPICE, Python, MATLAB, or measurement.

3. Physical Model of the RC Network

Consider a first-order RC low-pass network. A voltage source drives a series resistor R. The output node is shunted to the reference node by a capacitor. The output voltage is the voltage across the capacitor.

Let the input signal contain a DC bias and a sinusoidal component:

$$v_{in}(t) = V_b + A\cos(\omega t).$$

Here V_b is the bias voltage, A is the signal amplitude, and ω is the angular frequency. Write the capacitor voltage as

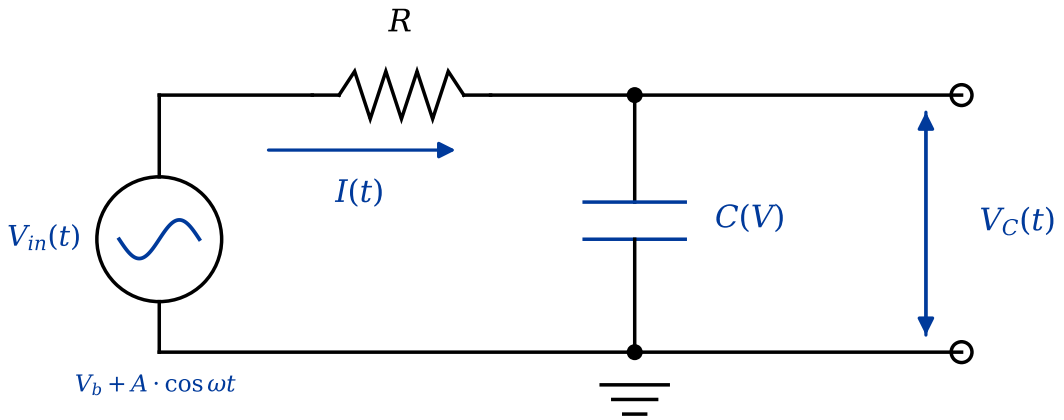

Figure 1: First-order RC low-pass network with a voltage-dependent shunt capacitor. The resistor is shown with the American zig-zag symbol.

$$v_C(t) = V_b + v(t),$$

where $v(t)$ is the AC component around the bias point.

If the capacitor were linear, its current would be $C\,dv_C/dt$. For a nonlinear capacitor, however, the fundamental state variable is charge. We therefore describe the capacitor by

$$Q = Q(v_C).$$

The capacitor current is

$$i_C(t) = \frac{dQ(v_C)}{dt}.$$

The resistor current is

$$i_R(t) = \frac{v_{in}(t) - v_C(t)}{R}.$$

Since the resistor current equals the capacitor current,

$$\frac{v_{in}(t) - v_C(t)}{R} = \frac{dQ(v_C)}{dt}.$$

Multiplying by R gives the charge equation in the original variables:

$$R\frac{dQ(v_C)}{dt} + v_C(t) = v_{in}(t).$$

After substituting $v_C(t) = V_b + v(t)$ and $v_{in}(t) = V_b + A\cos(\omega t)$, the DC terms cancel. The exact working equation is

$$R\frac{dQ(V_b+v)}{dt}+v(t)=A\cos(\omega t). \qquad (1)$$

Equation (1) is the starting point for the rest of the analysis. Its important feature is that it contains no artificial "instantaneous capacitance" element. All nonlinearity is contained in the charge function.

4. Expansion of the Differential Capacitance

To obtain analytical formulas, the charge-voltage relation must be approximated locally around the operating point. It is more convenient to do this through the differential capacitance:

$$C_d(V)=\frac{dQ(V)}{dV}.$$

Expand $C_d(V)$ in a Taylor series around the bias point V_b. Since $v_C(t)=V_b+v(t)$, the expansion is in powers of the AC voltage $v(t)$:

$$C_d(V_b+v)=C_0\left(1+a_1v+a_2v^2+a_3v^3+a_4v^4+...\right), \qquad (2)$$

where

$$C_0=C_d(V_b).$$

The coefficients a_1, a_2, a_3, a_4 are normalized derivatives of the differential capacitance:

$$a_1=\frac{1}{C_0}\left.\frac{dC_d}{dV}\right|_{V_b},$$

$$a_2=\frac{1}{2C_0}\left.\frac{d^2C_d}{dV^2}\right|_{V_b},$$

$$a_3=\frac{1}{6C_0}\left.\frac{d^3C_d}{dV^3}\right|_{V_b},$$

$$a_4=\frac{1}{24C_0}\left.\frac{d^4C_d}{dV^4}\right|_{V_b}.$$

The coefficient a_1 is the local normalized slope of the differential capacitance at the bias point. In other words, for a small voltage change v, the first-order relative change in capacitance is a_1v.

If $a_1\neq 0$, positive and negative voltage excursions from the bias point see different differential capacitance values. This local asymmetry is the source of the second harmonic.

The coefficient a_2 describes the local curvature of $C_d(V)$ at the bias point and is associated with the third harmonic. Higher coefficients contribute to the fourth, fifth, and higher harmonics.

Now use the relation between current and charge:

$$\frac{dQ}{dt} = C_d(V_b + v)\dot{v}.$$

Substituting the expansion of $C_d(V_b + v)$ gives

$$\frac{dQ}{dt} = C_0 \left(1 + a_1 v + a_2 v^2 + a_3 v^3 + a_4 v^4 + ...\right) \dot{v}.$$

Define the small-signal time constant

$$\tau = RC_0.$$

The circuit equation becomes

$$\tau\dot{v} + v + \tau a_1 v\dot{v} + \tau a_2 v^2\dot{v} + \tau a_3 v^3\dot{v} + \tau a_4 v^4\dot{v} + ... = A\cos(\omega t). \qquad (3)$$

Equation (3) is the central model used in this paper. It shows that the capacitor nonlinearity does not appear as a static nonlinear voltage function. It appears as the product of a voltage power and the voltage derivative.

This makes the physics different from a static nonlinearity such as $y = v + \alpha v^2$. For a static nonlinearity, the harmonic content is generated directly by the nonlinear input-output curve and is then filtered. Here the generation of the nonlinear current itself contains a time derivative, so the creation of harmonics is frequency dependent from the start.

One structural property of the nonlinear terms is useful. Every product $v^m\dot{v}$ is a total time derivative:

$$v^m\dot{v} = \frac{1}{m+1}\frac{d}{dt}\left(v^{m+1}\right). \qquad (4)$$

It follows from (4) that, for any periodic solution $v(t)$, the average value of each nonlinear combination over one period is zero:

$$\left\langle v^m\dot{v}\right\rangle_T = 0. \qquad (5)$$

The physical meaning of (5) is that the nonlinear capacitive current does not create a DC current component in the circuit. Over a full period, the charge taken up by the capacitor is returned. This is a direct consequence of the charge-conserving formulation. It should not be confused with the incorrect model $Q = C(V)V$, where the specified $C(V)$ is already meant to be a differential capacitance. In that model, the actual differential capacitance becomes $C(V) + VdC/dV$, which changes the physical problem [7], [8].

Since the AC part of the input contains no DC term, averaging the full equation over one period also gives

$$\left\langle v(t)\right\rangle_T = 0.$$

In Fourier-coefficient form, this means $c_0 = 0$.

5. Linear Response as the Reference Solution

Before calculating harmonics, recall the linear response of the RC network. Define the normalized angular frequency

$$\Omega = \omega\tau.$$

The quantity Ω is dimensionless. Since ω has units of s^{-1} and τ has units of seconds, their product is unitless.

The cutoff frequency of the linear RC low-pass network is

$$f_c = \frac{1}{2\pi\tau},$$

so

$$\Omega = \omega\tau = 2\pi f\tau = \frac{f}{f_c}.$$

Keeping only the linear terms gives

$$\tau\dot{v} + v = A\cos(\omega t).$$

Write the solution in complex notation as

$$v_1(t) = \mathrm{Re}\left\{\hat{V}_1 e^{j\omega t}\right\}.$$

Substitution gives

$$\hat{V}_1 = \frac{A}{1 + j\Omega}. \qquad (6)$$

The amplitude of the fundamental component across the capacitor is

$$|\hat{V}_1| = \frac{A}{\sqrt{1 + \Omega^2}}.$$

Result (6) appears throughout the following derivations. It shows that the capacitor voltage is nearly equal to the input at low frequency and falls as $1/\Omega$ at high frequency.

This frequency dependence limits the growth of distortion. The nonlinear current contains a derivative, which tends to increase with frequency. At the same time, the voltage factors participating in the nonlinear products decrease. The result is a finite-frequency maximum.

6. Second Harmonic

Return to the small-nonlinearity equation (3). After the linear part $\tau\dot{v} + v$, the nonlinear additions are

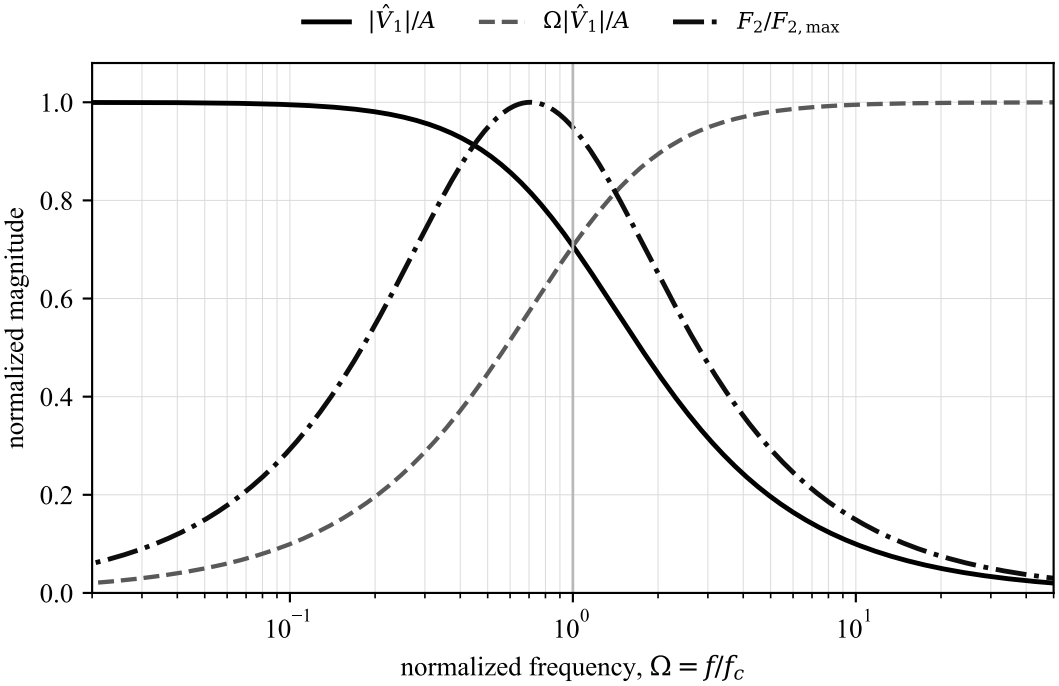

Figure 2: Competing frequency trends in the RC network. The capacitor voltage falls with frequency, the derivative-driven current term initially increases, and the distortion factor peaks at a finite normalized frequency.

$$\tau a_1 v\dot{v}, \quad \tau a_2 v^2\dot{v}, \quad \tau a_3 v^3\dot{v}, \ldots$$

To first order, the capacitor voltage is proportional to the input amplitude: $v_1 = O(A)$. Therefore $v_1\dot{v}_1 = O(A^2)$, while the next product $v_1^2\dot{v}_1$ is $O(A^3)$. The first nonlinear correction is therefore the term with coefficient a_1:

$$N_{2,\text{direct}}[v] = \tau a_1 v\dot{v}.$$

It is denoted $N_{2,\text{direct}}[v]$ because it is second order in signal amplitude and directly generates the second harmonic. At this order there is no cascade path to the second harmonic: no lower-order generated harmonic exists yet that could mix with the fundamental and produce 2ω. Physically, if the capacitance increases for one sign of the voltage excursion and decreases for the other, the charge and discharge waveforms are asymmetric. That asymmetry creates a component at twice the input frequency.

Use the linear solution $v_1(t)$ as the first approximation. The equation for the second-order correction is

$$\tau\dot{v}_2 + v_2 = -\tau a_1 v_1\dot{v}_1.$$

The right-hand side is the second-harmonic excitation created by $N_{2,\text{direct}}[v]$.

If the linear voltage is written as $v_1(t) = B\cos(\omega t + \varphi)$, then

$$v_1\dot{v}_1 = -B^2\omega\cos(\omega t + \varphi)\sin(\omega t + \varphi) = -\frac{B^2\omega}{2}\sin(2\omega t + 2\varphi).$$

Thus the product $v_1\dot{v}_1$ contains a component at 2ω. Passing that component through the linear RC response at 2ω gives the complex amplitude of the second harmonic:

$$\hat{V}_2 = -\frac{ja_1\Omega}{2}\frac{\hat{V}_1^2}{1+j2\Omega}. \qquad (7)$$

Formula (7) shows the structure of the effect. The factor $j\Omega$ comes from the derivative $\dot{v}_1$ in the nonlinear current term $v_1\dot{v}_1$: differentiating $e^{j\omega t}$ gives $j\omega$, and multiplying by τ gives $j\Omega$. Therefore, at small Ω, the excitation of the second harmonic grows in proportion to the input frequency. The denominator $1+j2\Omega$ shows that the generated second harmonic is filtered by the RC network at 2ω. The factor $\hat{V}_1^2$ contains the attenuation of the fundamental voltage at ω.

The second-harmonic amplitude relative to the fundamental is

$$\frac{|H_2|}{|H_1|} = \frac{|\hat{V}_2|}{|\hat{V}_1|} = \frac{|a_1|A}{2}\frac{\Omega}{\sqrt{1+\Omega^2}\sqrt{1+4\Omega^2}}. \qquad (8)$$

It is useful to isolate the dimensionless frequency-dependent factor:

$$F_2(\Omega) = \frac{\Omega}{\sqrt{1+\Omega^2}\sqrt{1+4\Omega^2}}.$$

For $\Omega \ll 1$,

$$F_2(\Omega) \approx \Omega.$$

Thus the second harmonic initially rises almost linearly with frequency. This matches the intuitive idea that faster voltage change produces a larger nonlinear capacitive current.

For $\Omega \gg 1$,

$$F_2(\Omega) \approx \frac{1}{2\Omega}.$$

The distortion now decreases. The capacitor voltage has become small, and the second harmonic is also attenuated at 2ω.

The maximum is found from

$$\frac{dF_2}{d\Omega} = 0.$$

Differentiating the logarithm is convenient:

$$\ln F_2 = \ln\Omega - \frac{1}{2}\ln(1+\Omega^2) - \frac{1}{2}\ln(1+4\Omega^2).$$

Then

$$\frac{1}{\Omega} - \frac{\Omega}{1+\Omega^2} - \frac{4\Omega}{1+4\Omega^2} = 0.$$

After simplification,

$$\Omega^2 = \frac{1}{2}.$$

Therefore,

$$\Omega_{\text{max},H2} = \frac{1}{\sqrt{2}} \approx 0.707. \qquad (9)$$

In frequency units, the second-harmonic maximum occurs slightly below the small-signal cutoff frequency:

$$f_{\text{max},H2} \approx 0.707 f_c.$$

This is the first important analytical result. The second-harmonic peak is not a simulation artifact. It follows directly from the structure of the charge equation.

7. Third Harmonic

The third harmonic has two mechanisms.

The first mechanism is direct. It comes from

$$N_{3,\text{direct}}[v] = \tau a_2 v^2 \dot{v}.$$

This term represents the local curvature of the differential capacitance curve. Even if the characteristic is symmetric around the operating point and the second harmonic is suppressed, curvature remains and generates a third harmonic.

The second mechanism is cascaded. If $a_1 \neq 0$, the $a_1 v\dot{v}$ term first generates a second harmonic. The fundamental and second harmonic then mix through the same $a_1 v\dot{v}$ nonlinearity and create a component at 3ω. The third harmonic can therefore depend not only on a_2, but also on a_1^2.

Collecting all third-order terms gives

$$\hat{V}_3 = -\frac{\hat{V}_1^3}{4(1+j3\Omega)} \left[j a_2 \Omega + \frac{3a_1^2\Omega^2}{1+j2\Omega} \right]. \qquad (10)$$

In (10), the first term in brackets is the direct mechanism through a_2, and the second is the cascaded mechanism through a_1^2. The denominator $1 + j3\Omega$ is the linear filtering of the third harmonic at 3ω.

The amplitude ratio can be written as

$$\frac{|H_3|}{|H_1|} = \frac{|\hat{V}_3|}{|\hat{V}_1|} = \frac{A^2}{4(1+\Omega^2)\sqrt{1+9\Omega^2}} \left| j a_2 \Omega + \frac{3a_1^2\Omega^2}{1+j2\Omega} \right|. \qquad (11)$$

Expression (11) is important for interpreting measurements. If a third harmonic is observed, it should not automatically be attributed only to a_2. At an asymmetric operating point, the cascaded a_1^2 mechanism can be significant.

To locate the frequency maximum in a simple form, consider the symmetric case

$$a_1 = 0.$$

Only the direct term remains:

$$\frac{|H_3|}{|H_1|} = \frac{|a_2|A^2}{4} \frac{\Omega}{(1+\Omega^2)\sqrt{1+9\Omega^2}}.$$

The corresponding dimensionless frequency-dependent factor is

$$F_3(\Omega) = \frac{\Omega}{(1+\Omega^2)\sqrt{1+9\Omega^2}}.$$

For $\Omega \ll 1$, it again grows as Ω. For $\Omega \gg 1$, it falls faster than the second-harmonic factor:

$$F_3(\Omega) \approx \frac{1}{3\Omega^2}.$$

The faster high-frequency rolloff occurs because the third harmonic depends on a higher power of the capacitor voltage and is also filtered at 3ω.

The maximum of F_3 is found from

$$\frac{d}{d\Omega} \ln F_3 = 0.$$

Since

$$\ln F_3 = \ln \Omega - \ln(1+\Omega^2) - \frac{1}{2}\ln(1+9\Omega^2),$$

we obtain

$$\frac{1}{\Omega} - \frac{2\Omega}{1+\Omega^2} - \frac{9\Omega}{1+9\Omega^2} = 0.$$

After rearrangement,

$$18\Omega^4 + \Omega^2 - 1 = 0.$$

Thus,

$$\Omega_{\text{max},H3} = \sqrt{\frac{\sqrt{73}-1}{36}} \approx 0.458. \qquad (12)$$

The direct third-harmonic maximum therefore occurs below cutoff, but still in the transition region of the filter. If the cascaded a_1^2 contribution is strong, the exact peak frequency can shift. The main conclusion remains: the maximum occurs at a finite frequency on the order of f_c.

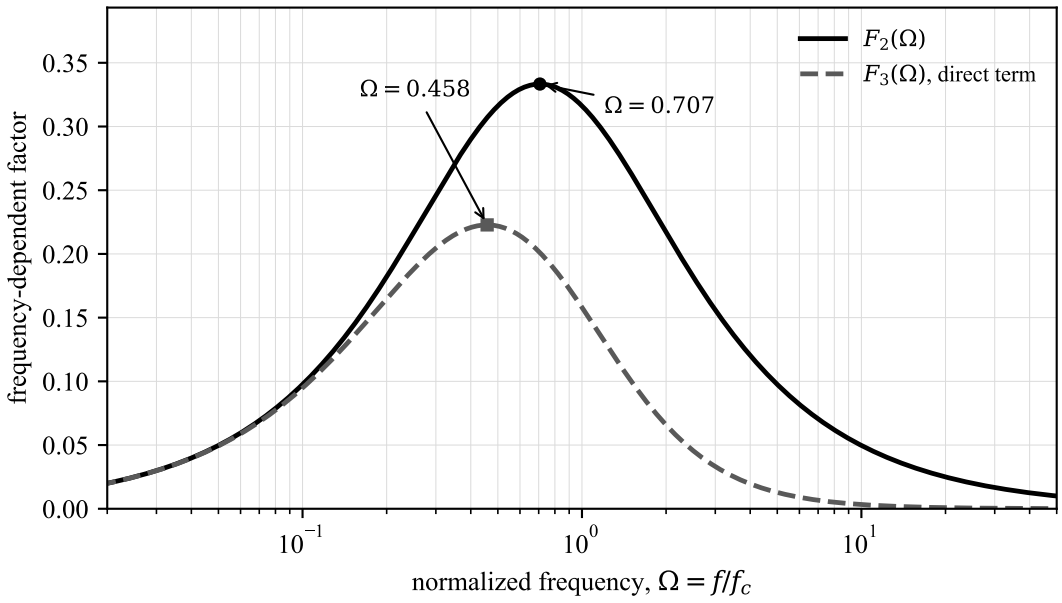

Figure 3: Frequency-dependent factors for the second harmonic and for the direct third-harmonic mechanism. The analytical maxima occur at $\Omega = 0.707$ and $\Omega = 0.458$, respectively.

8. Why a Recursive Form Is Useful for the Fourth and Fifth Harmonics

The second- and third-harmonic derivations are still compact enough to write by hand. For the fourth and fifth harmonics, the expressions quickly become bulky. The difficulty is not the circuit itself, but the number of cascaded paths.

For example, the fourth harmonic can be produced directly by a_3. It can also be produced by interaction between the fundamental and third harmonic, by the square of the second harmonic, and by mixing of the second harmonic with the fundamental through the $a_2 v^2 \dot{v}$ term. The fifth harmonic has still more paths: a direct a_4 contribution, interaction between the fundamental and fourth harmonic, interaction between the second and third harmonics, and additional paths through a_2 and a_3.

For higher harmonics, a recursive formulation is cleaner. Each new harmonic is expressed in terms of lower harmonics already obtained and the local coefficients of the nonlinearity. This is close in spirit to weakly nonlinear harmonic balance and Volterra-based distortion analysis used in analog circuits [10], [13].

Write the AC voltage as a Fourier series:

$$v(t) = \sum_{n=-\infty}^{\infty} c_n e^{jn\omega t}.$$

Since $v(t)$ is real,

$$c_{-n} = c_n^*.$$

The asterisk denotes complex conjugation. This condition means that the negative-frequency coefficient is not an independent physical component. Together with the positive-frequency coefficient, it forms a real sinusoidal component of the voltage.

Define

$$D_n = 1 + jn\Omega.$$

To first order, the fundamental coefficient is

$$c_1 = \frac{A}{2D_1}.$$

The physical amplitude of the n-th harmonic is $2|c_n|$, so harmonic ratios can be computed as

$$\frac{|H_n|}{|H_1|} = \frac{|c_n|}{|c_1|}.$$

In this notation, the second harmonic is

$$c_2 = -\frac{j\Omega}{D_2} a_1 c_1^2. \qquad (13a)$$

The third harmonic is

$$c_3 = -\frac{j\Omega}{D_3} \left(3a_1 c_1 c_2 + a_2 c_1^3\right). \qquad (13b)$$

These expressions are equivalent to the formulas derived above, but they are more convenient for continuing to c_4 and c_5. The following expressions are written to the first nonzero order in signal amplitude.

9. Fourth Harmonic

The fourth harmonic consists of three groups of terms.

The first group comes from the $a_1 v\dot{v}$ nonlinearity. It mixes the fundamental with the third harmonic and the second harmonic with itself:

$$S_{4,1} = a_1(4c_1 c_3 + 2c_2^2).$$

The second group comes from $a_2 v^2 \dot{v}$. It mixes two fundamentals and one second-harmonic component:

$$S_{4,2} = 4a_2 c_1^2 c_2.$$

The third group is the direct $a_3 v^3 \dot{v}$ contribution:

$$S_{4,3} = a_3 c_1^4.$$

After filtering by the linear RC response at 4ω,

$$c_4 = -\frac{j\Omega}{D_4}\left[S_{4,1} + S_{4,2} + S_{4,3}\right].$$

Equivalently,

$$c_4 = -\frac{j\Omega}{D_4}\left[a_1(4c_1c_3 + 2c_2^2) + 4a_2c_1^2c_2 + a_3c_1^4\right]. \qquad (14)$$

Thus,

$$\frac{|H_4|}{|H_1|} = \frac{|c_4|}{|c_1|}.$$

Formula (14) is useful not only for calculating the fourth harmonic, but also for understanding its origin. If a fourth harmonic appears in measurement, it should not be attributed only to a fourth-order term in the capacitance expansion. It can be produced by cascaded lower-order nonlinearities, especially when the second harmonic is strong.

10. Fifth Harmonic

The fifth harmonic is even more diagnostic because it involves all coefficients a_1, a_2, a_3, a_4.

The coefficient a_1 mixes the fundamental with the fourth harmonic and the second with the third. The coefficient a_2 contributes through combinations such as $c_1^2c_3$ and $c_1c_2^2$. The coefficient a_3 mixes three fundamentals with one second-harmonic term. The coefficient a_4 gives the direct fifth-order contribution.

The recursive form is

$$c_5 = -\frac{j\Omega}{D_5}\left[a_1(5c_1c_4 + 5c_2c_3) + a_2(5c_1^2c_3 + 5c_1c_2^2) + 5a_3c_1^3c_2 + a_4c_1^5\right]. \qquad (15)$$

The fifth-harmonic ratio is

$$\frac{|H_5|}{|H_1|} = \frac{|c_5|}{|c_1|}.$$

Formula (15) shows why higher harmonics can be useful for diagnostics but are difficult to interpret directly. The fifth harmonic contains information about the fourth derivative of the differential capacitance, but it also depends on all lower derivatives through cascaded mechanisms.

11. General Recursive Form

The expressions for c_2, c_3, c_4, c_5 are special cases of a general rule. If

$$v(t) = \sum_{n=-\infty}^{\infty} c_n e^{jn\omega t},$$

then the n-th Fourier coefficient of $v^m \dot{v}$ is the convolution

$$(v^m \dot{v})_n = \sum_{p_1+\ldots+p_m+k=n} jk\omega \, c_{p_1} \ldots c_{p_m} c_k. \qquad (16)$$

Substitution into the nonlinear equation gives

$$D_n c_n + \tau \sum_{m\geq 1} a_m (v^m \dot{v})_n = \frac{A}{2} \left(\delta_{n,1} + \delta_{n,-1} \right). \qquad (17)$$

For $n \geq 2$, the right-hand side is zero, so

$$c_n = -\frac{\tau}{D_n} \sum_{m\geq 1} a_m (v^m \dot{v})_n. \qquad (18)$$

Equation (18) is the general recursive harmonic-balance form. It can be used not only for H2 through H5, but also for higher-order harmonics. In practical small-nonlinearity calculations, the already-computed lower harmonics are substituted successively.

12. Main Physical Result

The main result can now be stated in simple circuit terms.

Harmonic distortion in an RC network with a voltage-dependent capacitor occurs because the capacitor charge is a nonlinear function of voltage. But the nonlinearity enters through current, meaning through dQ/dt. At very low frequency, distortion is small because the capacitor voltage is large but changes slowly.

At very high frequency, the opposite happens. The derivative could be large, but the voltage across the capacitor is strongly attenuated by the RC network. The generated harmonics also appear at 2ω, 3ω, 4ω, and 5ω, where the same filter attenuates them further.

Therefore, the largest distortion occurs in the middle. It appears near the small-signal cutoff frequency. For the second harmonic, the analytical maximum is

$$f \approx 0.707 f_c.$$

For the direct third-harmonic mechanism, the maximum is near

$$f \approx 0.458 f_c.$$

For the fourth and fifth harmonics, the exact peak frequency depends on the relative values of a_1, a_2, a_3, a_4, because cascaded mechanisms become important. The general principle remains: the maximum occurs at a finite frequency and is tied to the transition region of the RC filter.

This result matters in practical design. If a Class II MLCC is used in an RC filter and the useful signal band reaches the region near f_c, distortion can be worst exactly where the filter is still part of the signal path. A check at only low frequency or only small signal may miss the problem.

13. Connection to Real Class II MLCCs

The theory applies to any nonlinear capacitor that can be described by $Q(V)$ or $C_d(V)$. Its most important practical application is Class II MLCCs.

In a real X7R or X5R capacitor, $C_d(V)$ is not a simple polynomial. It can depend on package size, voltage rating, temperature, frequency, aging, and manufacturer [4], [5], [6]. Locally, however, over the operating signal range, it can be expanded in a series. The coefficients a_1, a_2, a_3, a_4 then connect the component characteristic to the measured distortion spectrum.

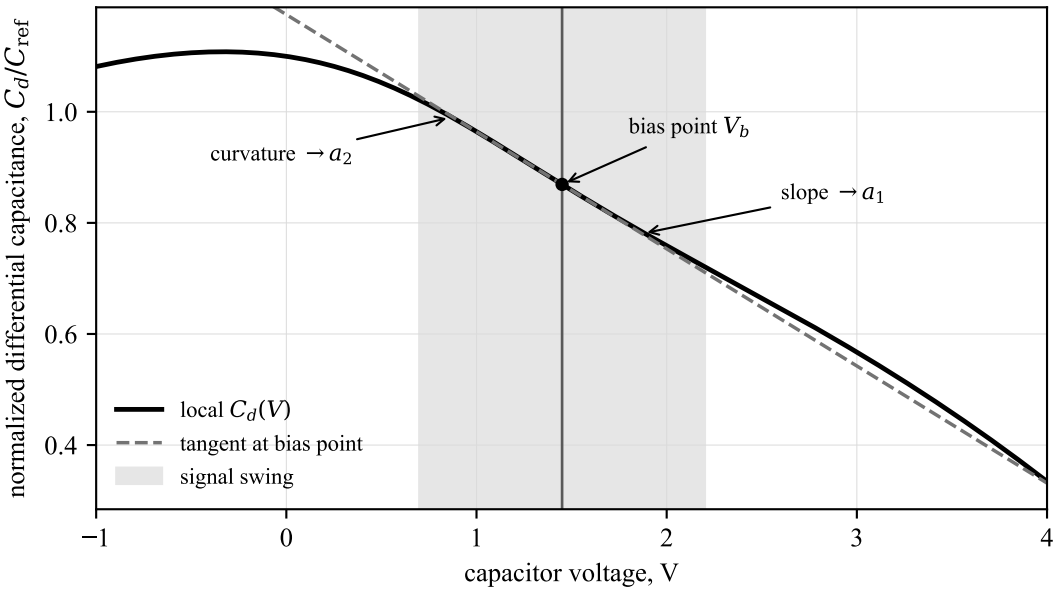

Figure 4: Illustrative local expansion of differential capacitance around the bias point. The slope contributes to a_1, the curvature contributes to a_2, and the shaded region indicates the signal swing. This is a conceptual sketch, not measured device data.

DC bias is especially important. If the capacitor operates near zero voltage and its characteristic is symmetric, a_1 may be small. The second harmonic is then suppressed, and the third harmonic may dominate. If the capacitor operates with DC bias, for example in a single-ended ADC input path biased around 2.5 V, the operating point moves to an asymmetric part of $C_d(V)$. Then a_1 becomes nonzero and the second harmonic can dominate.

Signal amplitude is also critical. To first order, the second harmonic is proportional to A, the third to A^2, the fourth roughly to A^3, and the fifth roughly to A^4 for the direct terms. A small-signal test may look acceptable while a full-scale signal produces unacceptable distortion.

14. Practical Design Implications

The analytical model leads to several direct engineering rules.

First, Class II MLCCs should not be used in critical signal-path nodes where low THD is required. If the capacitor sees a large AC voltage, use C0G/NP0, film, or another more linear dielectric [3], [4].

Second, reduce the voltage across the nonlinear capacitor. Because harmonic amplitudes fall rapidly with signal amplitude, even a moderate reduction in voltage swing can produce a large reduction in distortion.

Third, pay attention to the operating point. When possible, avoid placing a signal-path capacitor under strong DC bias. Moving the operating point to an asymmetric part of $C_d(V)$ increases the second harmonic.

Fourth, do not place the RC cutoff frequency near the top of the useful signal band without checking distortion if the capacitor is nonlinear. The distortion maximum can occur in that region.

Fifth, model the component correctly. Small-signal AC analysis does not show harmonic distortion. Time-domain simulation must use a charge-conserving $Q(V)$ model. Otherwise the simulated spectrum can reflect modeling errors as much as circuit behavior [7], [8].

15. Limits of the Theory

The theory is a small-nonlinearity theory. It assumes that a local expansion of the differential capacitance describes the component well over the operating signal range. This requires

$$\begin{aligned} |a_1 A| &\ll 1, \\ |a_2 A^2| &\ll 1, \\ |a_3 A^3| &\ll 1, \\ |a_4 A^4| &\ll 1. \end{aligned} \tag{19}$$

If the signal is too large or $C_d(V)$ is too nonlinear, the analytical formulas remain useful for understanding the mechanism, but accurate prediction should use the full charge model.

A second limitation is that the model assumes an instantaneous $Q(V)$ relation and an ideal external network. In real ceramic capacitors, capacitance can vary with DC bias, AC bias, temperature, frequency, aging, package size, and manufacturer [4], [5], [6]. In addition, real parts have nonideal effects not included in the $Q(V)$ model: dielectric absorption, leakage, ESR, ESL, self-resonance, and mounting parasitics [15], [16], [17], [18]. These effects can change the distortion spectrum, especially at high frequency. The present model should therefore be treated as a baseline charge-domain theory, not as a complete model of a specific MLCC.

A third limitation is the excitation type. This paper considers a single-tone sinusoidal input. For multitone signals, pulsed currents, or broadband noise, intermodulation products must be analyzed. The basic mechanism is the same: a nonlinear charge-storage element mixes frequency components through the dynamic relation dQ/dt.

Finally, the RC network is a continuous-time model. In a SAR ADC, the input process is sampled: there is a finite acquisition time, a switched sampling capacitor, charge injection, and memory of previous samples [11], [12], [14]. The present theory should therefore be viewed as a fundamental layer that can be extended to sampled-data systems.

16. Conclusion

This paper developed an analytical theory of harmonic distortion in an RC network with voltage-dependent capacitance. Unlike a shortcut based on instantaneous capacitance, the analysis uses a charge-conserving formulation. The capacitor is described by $Q(V)$, the differential capacitance is $C_d(V) = dQ/dV$, and the current is dQ/dt.

After expanding $C_d(V)$ around the bias point, the small-nonlinearity equation (3) is obtained. The nonlinearity is dynamic: the terms $v\dot{v}$, $v^2\dot{v}$, $v^3\dot{v}$, and $v^4\dot{v}$ generate the second, third, fourth, and fifth harmonics. Their frequency behavior is controlled by the balance between the increasing voltage derivative and the decreasing voltage across the capacitor due to the RC filter.

For the second harmonic, the maximum occurs at $\Omega = 1/\sqrt{2}$, or approximately $0.707 f_c$, as shown in (9). For the direct third-harmonic mechanism, the maximum is near $0.458 f_c$, as shown in (12). For the fourth and fifth harmonics, the recursive forms (14) and (15) show the contributions of direct and cascaded mechanisms.

The main result is that the harmonic-distortion maximum in an RC network with a nonlinear capacitor is a natural consequence of charge dynamics. It should not be expected at arbitrarily high frequency. It occurs in the transition region of the filter, where both the capacitor voltage and the capacitor current are significant.

The theory can be used as a foundation for further work on Class II MLCCs in precision analog circuits, SAR ADC front ends, anti-alias filters, AC-coupling networks, and power systems with pulsed currents. It also provides a basis for measurement methods, simulation models, and circuit techniques aimed at reducing distortion caused by voltage-dependent capacitance.

Appendix A. Derivation of the Recursive Formula

To obtain the higher harmonics, write the solution as

$$v(t) = \sum_{n=-\infty}^{\infty} c_n e^{jn\omega t}.$$

Then

$$\dot{v}(t) = \sum_{n=-\infty}^{\infty} jn\omega c_n e^{jn\omega t}.$$

The coefficient of $e^{jn\omega t}$ in $v^m\dot{v}$ is

$$(v^m\dot{v})_n = \sum_{p_1+\ldots+p_m+k=n} jk\omega\, c_{p_1} \ldots c_{p_m} c_k.$$

Substitution into the nonlinear equation gives

$$D_n c_n + \tau \sum_{m\geq 1} a_m (v^m\dot{v})_n = \frac{A}{2}\left(\delta_{n,1} + \delta_{n,-1}\right),$$

where

$$D_n = 1 + jn\Omega.$$

For $n \geq 2$,

$$c_n = -\frac{\tau}{D_n} \sum_{m \geq 1} a_m (v^m \dot{v})_n .$$

This is the general recursive harmonic-balance formula. It is useful for H2 through H5 and for higher-order harmonics as well.

Appendix B. Working Bibliography

[1] J. Caldwell, “Signal distortion from high-K ceramic capacitors,” *EDN*, 2013.
URL: https://www.edn.com/signal-distortion-from-high-k-ceramic-capacitors/

[2] EE News Europe, “More about understanding the distortion mechanism of high-K MLCCs,” *EE News Europe*, Dec. 22, 2013.
URL: https://www.eenewseurope.com/en/more-about-understanding-the-distortion-mechanism-of-high-k-mlccs/

[3] Z. Kaye, “Selecting Capacitors to Minimize Distortion in Audio Applications,” *Texas Instruments Analog Design Journal*, SLYT796A, Rev. A, 2020.
URL: https://www.ti.com/lit/pdf/slyt796

[4] Murata Manufacturing Co., Ltd., “Does the capacitance change when a DC voltage is applied to ceramic capacitors? Are there any points to be aware of regarding changes in the capacitance?”
URL: https://www.murata.com/support/faqs/capacitor/ceramiccapacitor/char/0005

[5] Murata Manufacturing Co., Ltd., “The voltage characteristics of electrostatic capacitance.”
URL: https://article.murata.com/en-global/article/voltage-characteristics-of-electrostatic-capacitance

[6] S. Cen, “DC Bias Characteristics of Ceramic Capacitors,” *KYOCERA AVX Technical Information*.
URL: https://www.kyocera-avx.com/docs/techinfo/CeramicCapacitors/mlcc-dc-bias-characteristics.pdf

[7] I. Zeltser and S. Ben-Yaakov, “On SPICE Simulation of Voltage-Dependent Capacitors,” *IEEE Transactions on Power Electronics*, 2018.
URL: https://cris.bgu.ac.il/en/publications/on-spice-simulation-of-voltage-dependent-capacitors/

[8] K. Kundert, “Modeling Varactors,” *The Designer’s Guide Community*.
URL: https://designers-guide.org/modeling/varactors.pdf

[9] D. E. Ward and R. W. Dutton, “A Charge-Oriented Model for MOS Transistor Capacitances,” *IEEE Journal of Solid-State Circuits*, vol. 13, no. 5, pp. 703-708, Oct. 1978.
URL: https://doi.org/10.1109/JSSC.1978.1051123

[10] P. Wambacq and W. Sansen, *Distortion Analysis of Analog Integrated Circuits*, Kluwer Academic Publishers, 1998.
URL: https://link.springer.com/book/10.1007/978-1-4757-5003-4

[11] IEEE Std 1241-2023, “IEEE Standard for Terminology and Test Methods for Analog-to-Digital Converters.”
URL: https://standards.ieee.org/ieee/1241/6797/

[12] M. Oljaca and K. Sanborn, “Determining Minimum Acquisition Times for SAR ADCs When a Step Function is Applied to the Input,” Texas Instruments Application Report SBAA173A, 2010.
URL: https://www.ti.com/lit/pdf/sbaa173

[13] J. Yang and S. X.-D. Tan, “Nonlinear Transient and Distortion Analysis via Frequency Domain Volterra Series,” *Circuits, Systems, and Signal Processing*, vol. 25, no. 3, pp. 295-314, 2006.
URL: https://intra.ece.ucr.edu/~stan/papers/cssp06.pdf

[14] B. F. Kuznetsov, “Voltage-Dependent Ceramic Capacitors as a Source of Dynamic Error in SAR ADC Front Ends: Charge-Conserving Modeling, Simulation Pitfalls, and ENOB Degradation,” *engrxiv* preprint, 2026.
URL: https://engrxiv.org/preprint/view/7456

[15] S. Guinta, “Ask The Applications Engineer-21: Capacitance And Capacitors,” *Analog Dialogue*, Analog Devices, Apr. 1996.
URL: https://www.analog.com/en/resources/analog-dialogue/articles/capacitance-and-capacitors.html

[16] Murata Manufacturing Co., Ltd., “What are impedance/ESR frequency characteristics in capacitors?”
URL: https://article.murata.com/en-global/article/impedance-esr-frequency-characteristics-in-capacitors

[17] KYOCERA AVX, “Parasitic Inductance of Multilayer Ceramic Capacitors,” Technical Information.
URL: https://kyocera-avx.com/docs/techinfo/CeramicCapacitors/parasitc.pdf

[18] AMD, “Capacitor Mounting Inductance,” *UltraScale Architecture PCB Design User Guide*, UG583.
URL: https://docs.amd.com/r/en-US/ug583-ultrascale-pcb-design/Capacitor-Mounting-Inductance